eXPRESS Polymer Letters Vol.14, No.9 (2020) 848–859
Available online at www.expresspolymlett.com
https://doi.org/10.3144/expresspolymlett.2020.70

Combination effects of reinforcing filler and impact modifier on the crystallization and toughening performances of poly(lactic acid)

N. Petchwattana[1*], *P. Naknaen*[2], *B. Narupai*[3]

[1]Division of Polymer Materials Technology, Faculty of Agricultural Product Innovation and Technology, Srinakharinwirot University, Ongkharak, 26120 Nakhon Nayok, Thailand
[2]Division of Food Science and Nutrition, Faculty of Agricultural Product Innovation and Technology, Srinakharinwirot University, Ongkharak, 26120 Nakhon Nayok, Thailand
[3]Expert Centre of Innovative Materials, Thailand Institute of Scientific and Technological Research, Khlong Luang, 12120 Pathumthani Thailand

Received 18 November 2019; accepted in revised form 21 February 2020

Abstract. In this research, poly(lactic acid) (PLA) was toughened and improved the crystallinity by rubber particles and inorganic filler. $CaCO_3$ was employed as a filler and nucleating agent while poly(methyl methacrylate)-poly(butadiene-styrene) (MBS) core-shell impact modifier was added as a toughening agent. Overall, the enhancements of both the toughness and crystallization of PLA with $CaCO_3$ and MBS were successfully achieved. The tensile modulus and strength of PLA increased with increasing $CaCO_3$ content from 10 to 30wt%. However, they decreased slightly when $CaCO_3$ loading reached 40 wt% due to particles agglomerations. With the addition of MBS rubber, the tensile modulus and strength of the PLA/$CaCO_3$ composites became lower than those observed for PLA/$CaCO_3$ composites due to the softening effect. Furthermore, the compositions with MBS showed superior toughness in terms of the tensile elongation at break and impact strength. $CaCO_3$ nucleated the PLA crystal which reflected as the increase in the degree of crystallinity (X_c) by at least 2 times for all formulations studied. The crystallization half-time ($t_{1/2}$) of PLA with 40 wt% $CaCO_3$ was dramatically reduced, from 26 min, in neat PLA, to 0.9 min. With the addition of MBS, it did at 2.7 min for the same $CaCO_3$ content. The maximum increment of heat distortion temperature (HDT), around 8 °C, was found for the PLA with 20 wt% $CaCO_3$.

Keywords: *polymer composites, impact modifier, nucleating agent, rubber toughening, crystallization*

1. Introduction

Poly(lactic acid) (PLA) is widely known as a commercially available, compostable thermoplastic, with mechanical properties comparable to many petroleum-based plastics such as poly(ethylene terephthalate) (PET) and polystyrene (PS) [1–15]. However, the problems of brittleness, low impact resistance, and high material cost still limit the applications of PLA as fossil-based polymers substitutions.

In terms of toughness, many elastic materials were applied as a toughening agent in PLA. Although their achievements of the impact strength and elongation at break were reported. However, these were found to simultaneously sacrifice the crystallinity, strength and thermal stability of PLA [1–6, 12–15]. PLA has been toughened by several toughening agents; *e.g.*, natural rubber, synthetic rubber, core-shell rubber (CSR) and other thermoplastics [1–2, 11–15]. For instance, with the presence of thermoplastic copolyester elastomer (TPCE), the impact strength of PLA was increased by six-fold when TPCE was added at 30 wt% [12]. Blending PLA with 20 wt% epoxidized

*Corresponding author, e-mail: nawadon@g.swu.ac.th

natural rubber (ENR) was found to increase the tensile elongation at break by three times while the impact strength increased by around five times [13]. Toughening PLA with 15 wt% poly(butyl acrylate) showed a drastic toughness improvement with the increased elongation at break from 4.52 to 174% while the impact strength increased from 2.13 to 47.02 MJ/m^3 [14]. With the addition of ultrafine, fully vulcanized, acrylate rubber (UFPR), the tensile elongation at break dramatically increased from 3.46 to 198% and the impact strength increased by around five times at 10 wt% UFPR. The UFPR was found to induce numerous crazes as a mechanism of energy absorption [15]. In our previous work, we found that adding CSR to PLA/wood composites resulted in the toughness increment. Mechanical tests indicated that toughening PLA/wood flour composites with 5 wt% CSR significantly improved both the impact strength and the tensile elongation at break. Compared to other toughening systems, CSR seemed to be a more appropriate toughening agent for PLA and PLA composites. It required lower amounts than other toughening agents to improve the toughness of PLA [1–3, 6, 15].

For the crystallinity and thermal stability point of view, previous literatures have indicated that adding inorganic fillers and natural fibers to PLA improved the degree of crystallinity, mechanical strength and thermal stability. However, the toughness reductions were also reported due to the brittle nature of PLA and the poor interfacial adhesion between PLA matrix and fillers. For example, the flexural strength and strain at break of PLA/$CaCO_3$ composites were found to be significantly reduced, especially when the filler loading was larger than 30 wt% [5]. The crystallization ability of PLA was found to significantly increase with the addition of talc. The authors concluded that in order to have PLA with good mechanical and thermal stability, both the presence of filler and PLA crystals are needed [17]. The tensile elongation at break and impact strength of the toughened PLA/rubber-wood sawdust composites were reduced with the wood flour loading due to their poor interfacial adhesion. With the addition of CSR, both the tensile elongation at break and impact strength were increased significantly [6]. With the presence of titanium dioxide, the elongation at break of PLA decreased by more than 1.5 times [7]. The problem of weak interfacial bonding is generally remedied by incorporating coupling agents, such as maleic anhydride-grafted PLA [8], silane coupling agent [9, 10] or epoxy-based coupling agent [11]. Although these chemicals have been reported to be effective as the interfacial adhesion promoters for PLA composites but they were less effective at high filler contents (more than 20 wt%) [8–11]. Thus, the improvement of the PLA composite toughness still needs a more appropriate method in the case of highly filled PLA composites.

In this work, PLA was toughened and crystal nucleated simultaneously. $CaCO_3$ was employed as a filler and nucleating agent while poly(methyl methacrylate)-poly(butadiene-styrene) (MBS) core-shell impact modifier was added as a toughening agent. Various tests were performed on PLA/$CaCO_3$ composites, with and without MBS, to evaluate the crystallization rate, mechanical performance and thermal stability.

2. Materials and methods

2.1. Materials

An injection grade of PLA (Ingeo™ Biopolymer 3001D, NatureWorks LLC, USA) was used as a polymer matrix. It has a density and melt flow index (MFI) of 1.23 g/cm^3 and 22 g/10 min, respectively. Fine particles of $CaCO_3$ were added to PLA to reduce the raw material cost, increase the crystallization rate and improve the stiffness of PLA. It has a density and average particle size of 2.71 g/cm^3 and 5 μm respectively. It was supplied by U&V Holding Co., Ltd., Thailand. The MBS, supplied by Farto Square Co. Ltd., was added to PLA/$CaCO_3$ composites to remedy the problem of brittleness. It has a bulk density and average particle size of 0.50 g/cm^3 and 500 nm respectively.

2.2. Preparation of PLA/$CaCO_3$ composites and MBS toughened PLA/$CaCO_3$ composites

Each raw material was firstly dried in a vacuum oven at 65 °C for 12 h to eliminate the inherent moisture. After that, the PLA was dry mixed with 10–40 wt% $CaCO_3$. The $CaCO_3$ compositions were then melt-compounded using a co-rotating, twin-screw extruder (CTE-D16L32, Charoen Tut Co. Ltd., Thailand) and pelletized to get the PLA/$CaCO_3$ composite pellets. The temperature profile of the extruder barrel was 160/175/185/190/185 °C. The PLA/$CaCO_3$ composite pellets were further dry- and then melt-extruded with 5 wt% MBS. Table 1 shows the composition

Table 1. Blend formulations of the raw materials.

Formulation code	PLA [wt%]	$CaCO_3$ [wt%]	MBS [wt%]
PLA	100	–	–
PC10	90	10	–
PC20	80	20	–
PC30	70	30	–
PC40	60	40	–
PC10M	85	10	5
PC20M	75	20	5
PC30M	65	30	5
PC40M	55	40	5

Table 2. Injection molding conditions.

Designation	Value
Mold closing and clamping	5 sec
Injection filling	10 sec
Injection pressure holding	15 sec
Cooling time	60 sec
Mold opening, de-clamping and ejecting	10 sec
Barrel temperature Zones 1 to 3	195/200/200 °C
Injection feed-forward pressures	40–80 bar
Holding pressure	30 bar
Mold clamping pressure	70 bar
Ejector pressure	30 bar
Mold temperature	40 °C

of the materials used in the current research. The pelletized formulations were all processed using an injection molding machine (INJ101T, Charoen Tut Co. Ltd., Thailand) to produce the test specimens. The injection molding conditions are shown in Table 2.

2.3. Testing and characterizations

Tensile tests were done at room temperature using a universal testing machine (INSTRON 5966, Instron Co., Ltd., USA) in accordance with ASTM D638. The crosshead speed was 50 mm/min and the gauge length was set at 1 in. The Izod impact strength of each of the PLA/$CaCO_3$ and PLA/$CaCO_3$/MBS composites was determined using an Izod impact tester (BPI-25 COM, Zwick Roell, Germany) following the procedure described in ASTM D256. The mechanical test results reported were the average values of five tested specimens.

The impact fracture surfaces of the neat PLA, PLA/$CaCO_3$, and PLA/$CaCO_3$/MBS composites were investigated using a field emission scanning electron microscope (FE-SEM) (JSM IT500HR, JEOL, Japan) at an accelerating voltage of 1.0 kV. The test specimens were placed on aluminum stubs and coated with a thin layer of gold before the FE-SEM study.

Differential scanning calorimetry (DSC) (DSC6000, PerkinElmer, Inc., USA) was performed on five to ten-milligram samples to observe the transition temperatures of the neat PLA, PLA/$CaCO_3$ and PLA/$CaCO_3$/MBS composites. The thermal scans started with heating from 0 to 200 °C at a ramp rate of 5 °C/min to remove the thermal history. The samples were held isothermally for 5 min at 200 °C and then cooled down to 0 °C at 5 °C/min and then held at 0 °C for 5 min. Finally, they were re-heated to 200 °C at the same heating rate; the first cooling and second heating scans were reported. The degree of crystallinity (X_c) due to the second heating was calculated by Equation (1):

$$X_c = 100 \cdot \frac{\Delta H_M - \Delta H_{CC}}{x_p \cdot \Delta H^0} \quad (1)$$

where ΔH_M, ΔH_{CC} and x_p are the enthalpy of melting, enthalpy of the cold crystallization, and the weight fraction of the PLA in the composites respectively. These values were obtained from the area under the DSC second heating thermograms. ΔH^0 is the heat of fusion obtained from the melting enthalpy of 100% crystalline PLA, which is 93 J/g [15–17].

The crystallization half time ($t_{1/2}$), at 100 °C, was determined using DSC isothermal scans. All the samples were heated from room temperature to 200 °C at 5 °C/min and then isothermally held at 200 °C for 5 min. They were cooled down to 100 °C at 5 °C/min and held isothermally at this temperature until the crystallization was completed.

The service temperature of the PLA composites was measured using a heat distortion tester (HV-3000-P3C, Gotech Testing Machines Inc., Republic of China) in accord with ASTM 648 with applied stress of 0.455 MPa. The measurements were conducted in silicone oil with a heating rate of 2 °C/min until the test specimen deflected 0.25 mm.

3. Results and discussions

3.1. Mechanical properties and microscopic observations

Figure 1 shows the modulus values of PLA/$CaCO_3$ composites with and without MBS. It was found that adding $CaCO_3$ into PLA leads to the increase of stiffness characterized by the Young's modulus by 15.0, 39.6, 54.2 and 57.2% for 10, 20, 30, and 40 wt%

$CaCO_3$ respectively. This indicated that $CaCO_3$ played a significant role of PLA stiffness improvement and deformability restriction at all concentrations [5, 7, 10]. With the addition of MBS, the tensile moduli were reduced at all $CaCO_3$ concentrations by 34.48, 39.69, 36.54 and 25.19% for PLA with 10, 20, 30, and 40 wt% $CaCO_3$ respectively. The decreased stiffness of PLA composites could be ascribed to the dispersed MBS particles which acted as a softener [18]. The tensile strengths of PLA filled with 10, 20, 30 and 40 wt% $CaCO_3$, with and without MBS, are graphically presented in Figure 2. $CaCO_3$ exhibited its reinforcing effects on PLA with the increase of the tensile strength when it was added from 10–30 wt%. We attributed the improved tensile strength to the good dispersion of $CaCO_3$ which facilitated the PLA-$CaCO_3$ stress transfer at this loading range. However, there was a slight drop of the tensile strength when $CaCO_3$ loading reached 40 wt% due to the agglomeration of the $CaCO_3$ particles (Figure 2b). Modifying the PLA/$CaCO_3$ composite with MBS was found to soften PLA composites with the reduction of the tensile strength by around 9–21% depending on $CaCO_3$ concentration due to the softening effects of the MBS rubber. Interestingly, there was a drop in the tensile strength when PLA-$CaCO_3$ loading reached 40 wt%. This was due to the lack of PLA-$CaCO_3$ stress transfer from the agglomerations, as shown by the FE-SEM micrographs in Figure 2c. The results of the tensile modulus and tensile

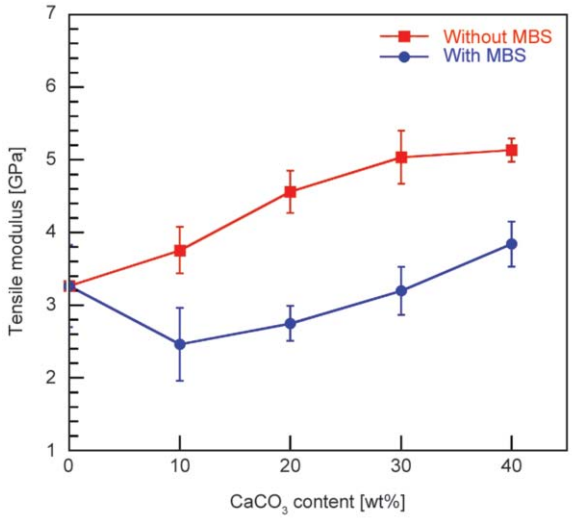

Figure 1. Tensile modulus of PLA/$CaCO_3$ composites with and without MBS.

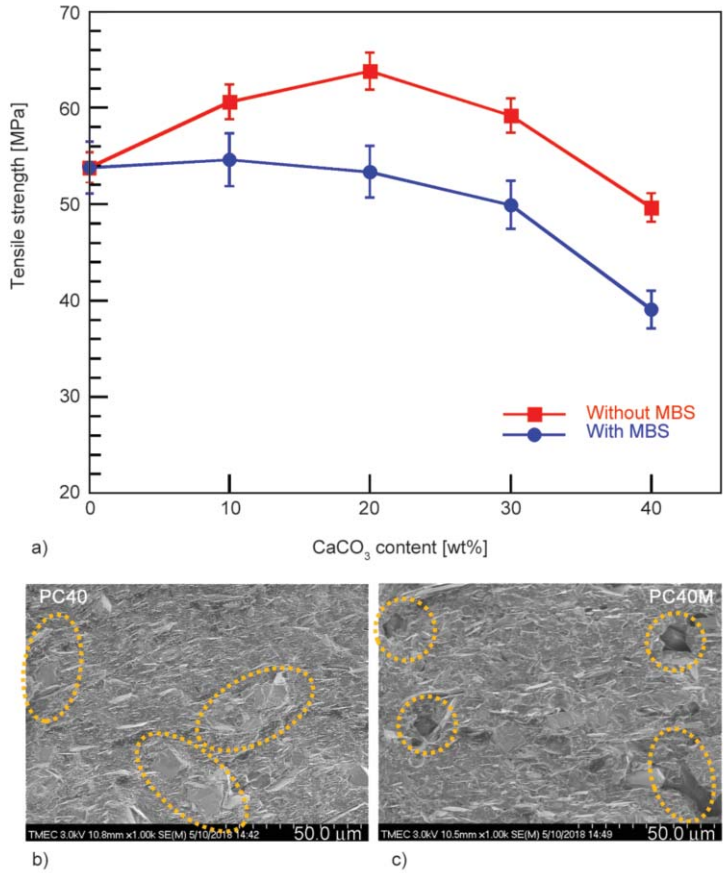

Figure 2. Tensile strength of PLA/$CaCO_3$ composites with and without MBS. a) tensile strength of PLA/$CaCO_3$ composites, b) FE-SEM micrograph of PC40 and c) FE-SEM micrograph of PC40M.

strength are in agreement with the previous reports. Kim *et al*. [19] found that the tensile modulus and strength of PLA increased with $CaCO_3$ only for low loadings of 5–10 wt%. Higher than these contents, their values dropped significantly. Kasuga *et al*. [5] showed that the increase of flexural strength of PLA was limited at 30 wt% of the vaterite form of $CaCO_3$. Beyond this content, it reduced drastically. As shown in Figure 3, the tensile elongation at break of PLA was 7.1% and it increased to 29.5% with the addition of 5 wt% MBS. For PLA/$CaCO_3$ composites, the tensile elongation at break gradually reduced at all concentrations and reached the minimum value of 1.8% at 40 wt% $CaCO_3$. This is attributed to the restriction of PLA chain entanglements induced by the $CaCO_3$ rigid particles during the tensile test [1, 20–21]. This phenomenon has generally been found in semi-crystalline polymer/inorganic filler composites. Kim *et al*. [19] reported that the elongation at break of PLA reduced from 4 to 1.9% with the addition of 30 wt% $CaCO_3$. Osman *et al*. [22] showed that with the incorporation of only 0.2 vol% $CaCO_3$, the elongation at break of low-density polyethylene (LDPE) was dramatically reduced from 617 to 17%. For PLA/$CaCO_3$ with MBS, the elongation at break of PLA/10 wt% $CaCO_3$ was found to increase significantly from 7.1%, in neat PLA, to nearly 24%. The FE-SEM micrograph, in Figure 3c, shows the well-dispersed and embedded MBS within the PLA matrix. These were the main reason for the improvement of the elongation at break at 10 wt% $CaCO_3$. Further addition of $CaCO_3$ at 40 wt% in PLA/$CaCO_3$/MBS was found to linearly reduce the elongation at break down to 6.38% due to the agglomerations and PLA chain entanglement restrictions. Moreover, the poor interfacial adhesion between PLA and $CaCO_3$ and the pulled-out $CaCO_3$ particles which initiated the cracks [23] during the tension process were the additional causes of the elongation at break reductions. Our previous work on the toughening of

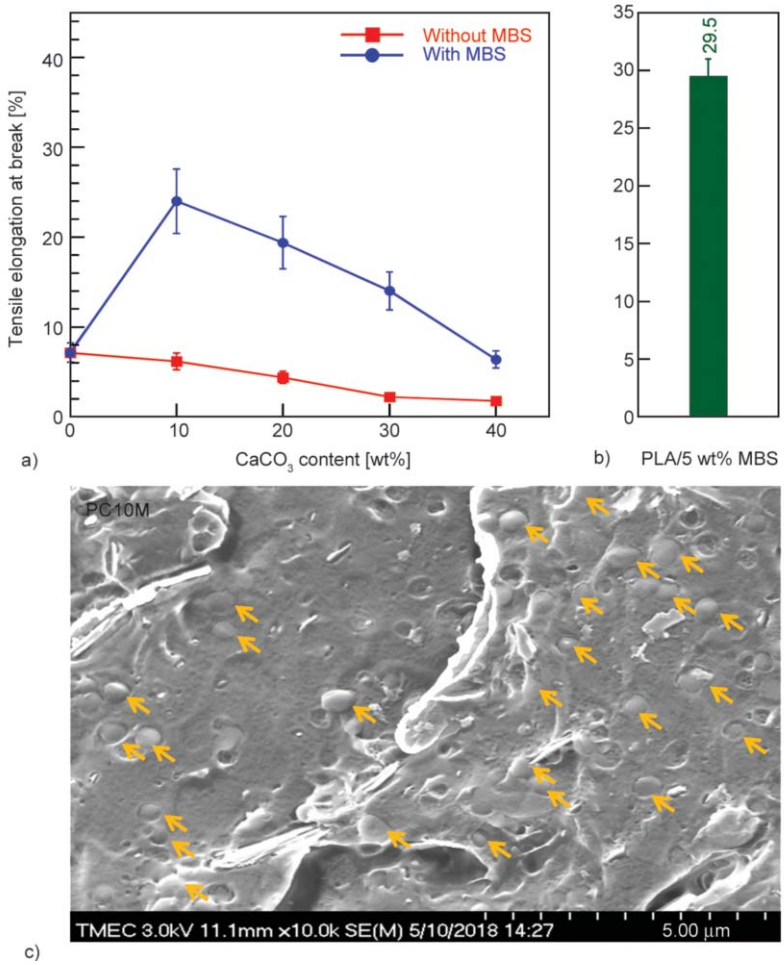

Figure 3. Tensile elongation at break of PLA/$CaCO_3$ composites with and without MBS. a) Tensile elongation at break of PLA/$CaCO_3$ composites, b) tensile elongation at break of PLA/5 wt% MBS and c) dispersion of MBS in PLA matrix (PC10M).

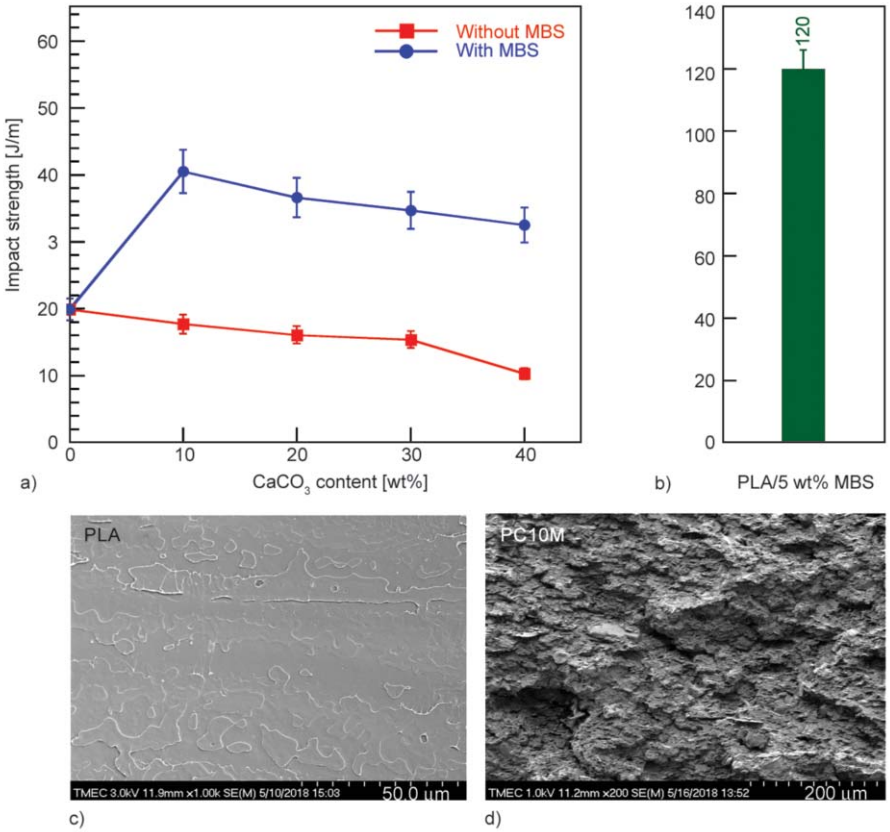

Figure 4. Impact strength of PLA/$CaCO_3$ composites with and without MBS. a) Impact strength of PLA/$CaCO_3$ composites, b) impact strength of PLA/5 wt% MBS, c) impact fracture surface of neat PLA and d) impact fracture surface of PC10M.

PLA/wood composites indicated that adding the acrylic impact modifier played an important role in the elongation at break improvement. FE-SEM micrographs of PLA/ acrylic impact modifier indicated some plastic deformations induced by the acrylic impact modifier together with the cavitations. These were the critical parameters for the toughness improvement for PLA/wood composites [6].

As shown in Figure 4a, the impact strength of PLA was around 20 J/m and the PLA/$CaCO_3$ composites, with and without MBS, behaved similarly to the tensile elongation at break. In Figure 4b, the PLA/MBS showed the impact strength of 120 J/m. For the PLA/$CaCO_3$ composites, the impact strength linearly decreased with increasing $CaCO_3$ filler especially at 40 wt%. For the composites with MBS, the impact strength was found to increase by around two times for all $CaCO_3$ loading. The inserted FE-SEM images in Figure 4c and 4d indicated some morphological differences between the neat PLA and PLA/$CaCO_3$/MBS composites. Neat PLA fractured with a very smooth surface which allowed the crack to propagate rapidly; low impact energy was required in this case. In Figure 4d, the composite with MBS (PC10M) showed a rough fracture surface which indicated that more energy was required to propagate the crack and break the specimen [1, 6, 15]. This result is in agreement with numerous reports. Battegazzore *et al*. [24] toughened PLA/ cotton fabric composites with polyhydroxybutyrate (PHB) and found the highest Charpy impact strength of 54.5 kJ/m^2. With the addition of the epoxidized natural rubber (ENR), the toughness of PLA/talc composites significantly increased more than ten times due to ENR concentration. The authors suggested that the ENR facilitated the mobility of PLA chains which allowed the PLA/talc/ENR composites to deform with difficulty during applied impact force [25].

3.2. Crystallization behavior

Figure 5 illustrates the DSC thermograms of the neat PLA and its composites with and without MBS obtained from the second heating scan. Further peak identifications and calculations are listed in Table 3. Neat PLA showed a T_g value of 61.9 °C. The incorporation of $CaCO_3$ slightly changed the T_g of PLA

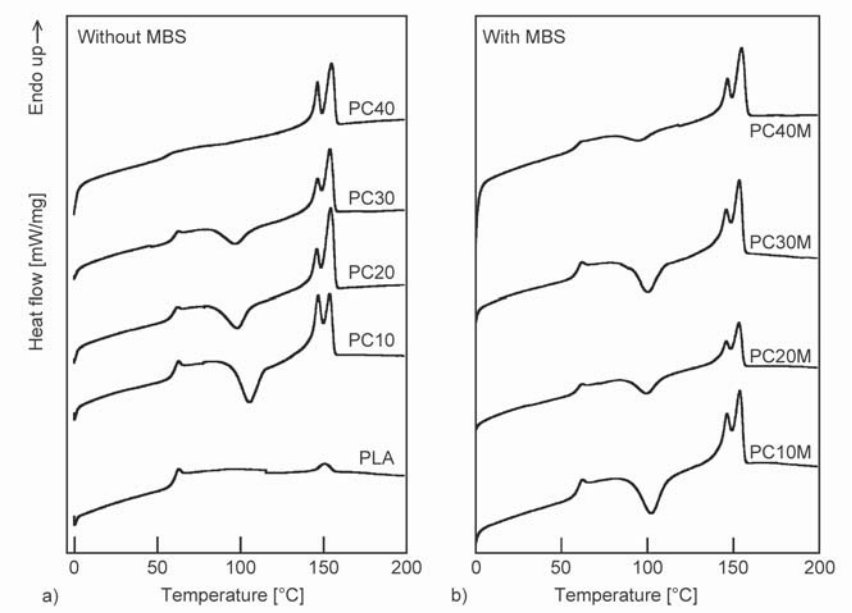

Figure 5. DSC second heating thermograms of the PLA/$CaCO_3$ composites a) without MBS and b) with MBS.

by around 1–2 °C for all compositions. The maximum T_g of 62.8 and 62.4 °C was observed in PC40 and PC40M respectively. This was generally reported in other nucleated PLA systems [17, 26].

The crystallization temperature is a parameter related to the crystallization rate of the polymer [27]. With the addition of a nucleating agent, a decrease of crystallization temperature upon cooling (T_{co}) refers to a slower crystallization rate whereas a decrease of crystallization temperature upon heating (T_{cc}) indicates a faster crystallization rate [27, 28]. As shown in Figure 5 and Table 3, the T_{cc} of PLA composites was significantly reduced by around 20 °C for all PLA/$CaCO_3$ and PLA/MBS/$CaCO_3$ compositions. This is attributed to the crystallization acceleration of the PLA by $CaCO_3$ and provided a benefit for the injection molding process. This crystallization enhancement was mainly due to the poor interfacial morphology of $CaCO_3$ in the PLA matrix as illustrated in Figure 6. The poor interfacial adhesion and voids around $CaCO_3$ particles were observed on both PLA composites with and without MBS. These incompatible phases induced thermal insulation zone which reduced the heat transfer from the PLA matrix to $CaCO_3$ particles and the temperature of the $CaCO_3$ particles remained lower than that of the PLA matrix. These cold spots turned into the crystal nuclei and then the PLA chains around these nuclei started to form crystals [27–31]. This made the whole PLA samples were crystallized at lower temperature. In comparison, the PLA/$CaCO_3$ composites showed slight-lower T_{cc} than that observed in PLA/$CaCO_3$/MBS composites with the same $CaCO_3$ content. This was due to the crystallization obstruction induced by MBS, as we previously reported [6, 31]. For T_m, single melting endotherm was observed at 150 °C in neat PLA. The addition of $CaCO_3$ did not significantly shift the T_m of PLA. With $CaCO_3$ filler, the T_m split into two peaks due to the less-perfect crystals formed by cold crystallization during the reheating process [32, 33]. For the polymer processing point of view, the T_{cc} data is usually used to describe the crystallinity data of the plastic injection molding process, annealing process or increase in the dimensional stability of plastic products. A lower T_{cc} indicates that less energy is required for the injection

Table 3. Thermal transition temperatures and degree of crystallinity of PLA/$CaCO_3$ composites with and without MBS obtained from the cooling and 2nd heating thermograms.

Formulation	T_{co} [°C]*	T_g [°C]**	T_{cc} [°C]**	T_{m1} [°C]**	T_{m2} [°C]**	X_c [%]**
PLA	n.d.	61.2	120	150	n.d.	8.30
PC10	92.8	61.9	105	146	153	21.7
PC20	95.2	62.2	97.0	145	154	22.8
PC30	97.1	62.0	97.2	145	153	23.8
PC40	99.3	62.8	96.4	143	152	24.3
PC10M	95.9	61.9	102	145	153	20.5
PC20M	95.8	61.3	99.6	145	153	18.6
PC30M	95.9	61.3	100	145	153	20.1
PC40M	95.2	62.4	108	146	154	22.3

*Obtained from the cooling thermogram
**Obtained from the 2nd heating thermogram
n.d. = no crystallization or melting peaks were detected

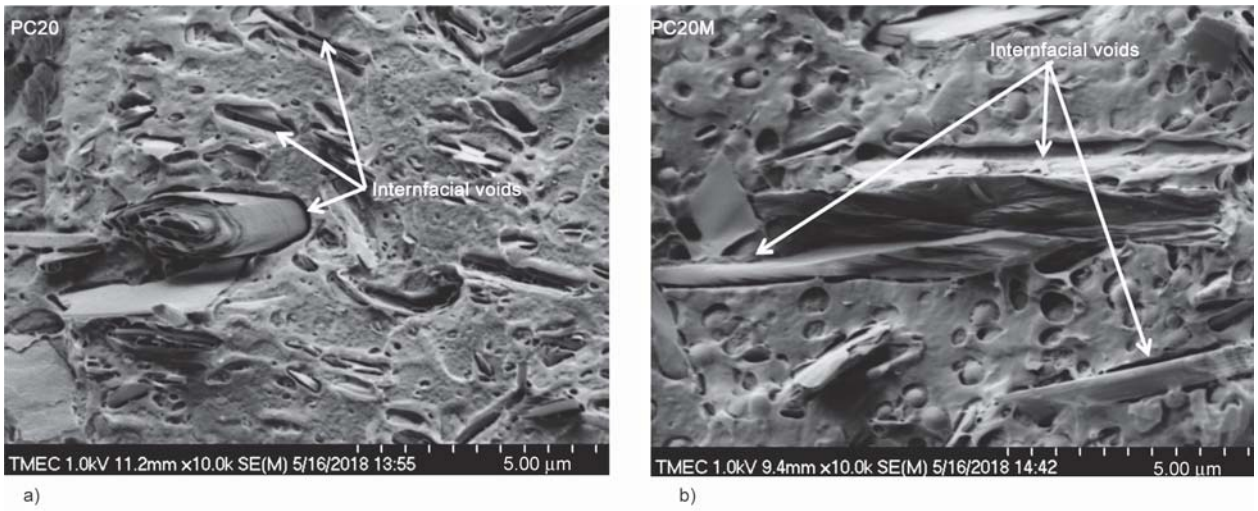

Figure 6. Fractured surfaces of the composites with 20 wt% $CaCO_3$ indicating the interfacial voids and cold spots of nucleations. a) PC20 and b) PC20M.

process since a lower temperature can be used [34, 35].

Figure 7 shows the cooling curves of PLA and its composites with and without MBS. For neat PLA, no crystallization peak was observed under this cooling condition. With the presence of $CaCO_3$, a single peak was observed at all loadings and the T_{co} tended to increase slightly with increasing $CaCO_3$ concentrations. For the PLA/$CaCO_3$ with MBS, no significant change in T_{co} was detected. These confirmed the nucleating ability of $CaCO_3$ for PLA crystallization and that obstruction was done by the MBS.

Table 3 shows some significant improvements in the degree of crystallinity (X_c) of the PLA composites with the addition of $CaCO_3$, which were calculated following Equation (1). The X_c increased significantly since $CaCO_3$ was added at 10 wt% and then slightly increased with further addition of the filler. The $CaCO_3$ particles are suggested to have promoted the crystal formation as well as accelerated the crystallization rate in PLA via the mechanism described above. This is similar to the results reported by Liang *et al*. [32]. With the addition of nano $CaCO_3$, the X_c of PLA increased from around 5 to 35% with only

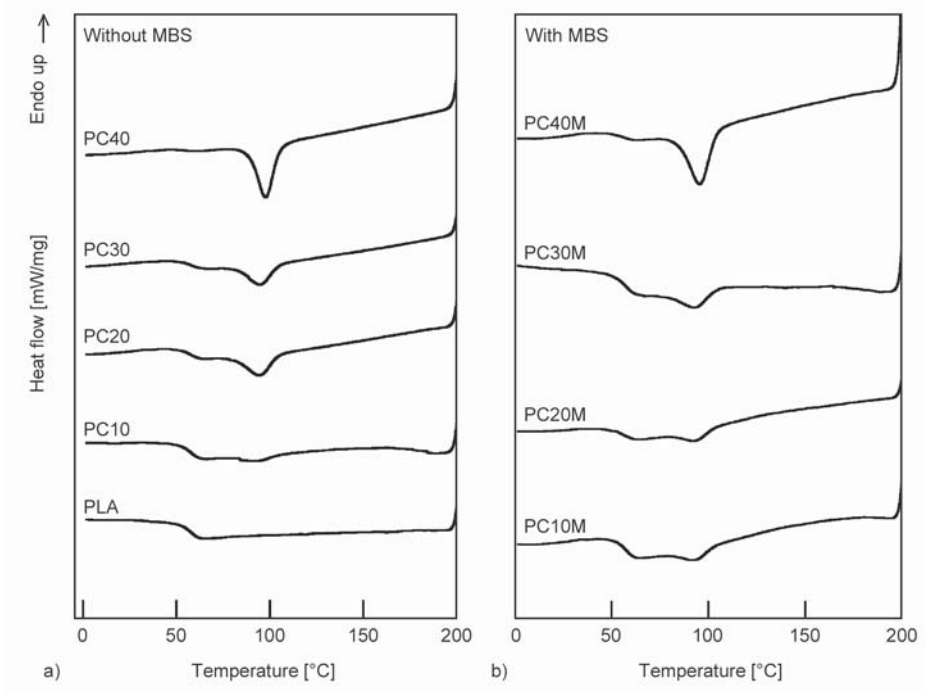

Figure 7. DSC cooling thermograms of the PLA/$CaCO_3$ composites a) without MBS and b) with MBS.

2 wt% filler added while the T_c reduced by around 10 °C. Our previous work indicated that with the addition of talc, the X_c of PLA increased from 3.6 to 30.9% [33]. Xia *et al*. [36] found that adding flax fiber to PLA increased the X_c by two times. Further observation indicated that the flax fiber reduced the crystal size of PLA and induced the formation of α-form crystals.

As shown in Figure 8, the $t_{1/2}$ values of PLA crystallized at 100 °C and the DSC isothermal peaks were dramatically reduced, from 26 to 0.9 min, with the addition of 40 wt% $CaCO_3$. For the composites with MBS, it decreased to 2.7 min at the same $CaCO_3$ loading. Technically, the crystallization rate is related to the free enthalpy of the crystal nuclei formation [27, 35, 37]. In this case, neat PLA had a high free enthalpy resulted in the PLA with a very slow crystallization rate. Adding $CaCO_3$ resulted in the decrease of this free enthalpy and enhanced the crystal nucleation at this tested temperature. These results are also similar to those observed in the previous literatures. The $t_{1/2}$ of the PLA/talc composites was reduced from 35 min down to 4 min with the addition of 10 wt% talc [27] while modifying PLA with dimethylbenzylidene sorbitol was found to reduce the crystallization time (t_c) from more than 40 to less than 5 min at the crystallization temperature of 100 °C [4].

3.3. Heat distortion temperature (HDT)

As shown in Figure 9, neat PLA exhibited the HDT value of 53.8 °C, and all the formulations showed higher HDT values than that observed in neat PLA. In PLA composites, it increased to 57.7, 61.3, 59.1 and 54.1 °C for PLA with 10, 20, 30 and 40 wt% $CaCO_3$ respectively. With the MBS toughening, it changed to 55.4, 56.9, 55.4, and 51.8 °C for PLA with 10, 20, 30 and 40 wt% $CaCO_3$ respectively. These increments were mainly due to the increased X_c and the reinforcement effect provided by the

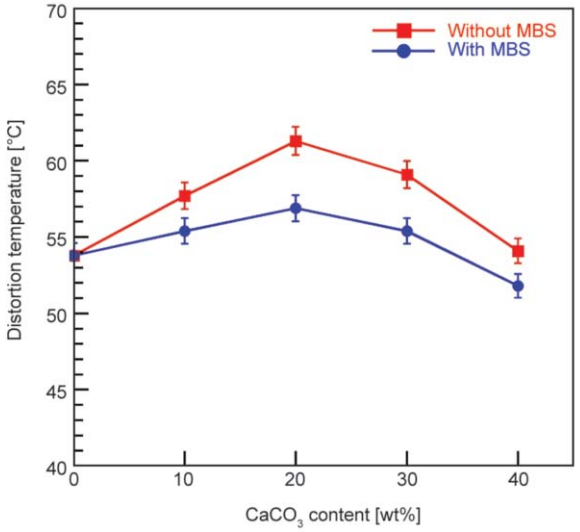

Figure 9. HDT of the PLA/$CaCO_3$ composites with and without MBS.

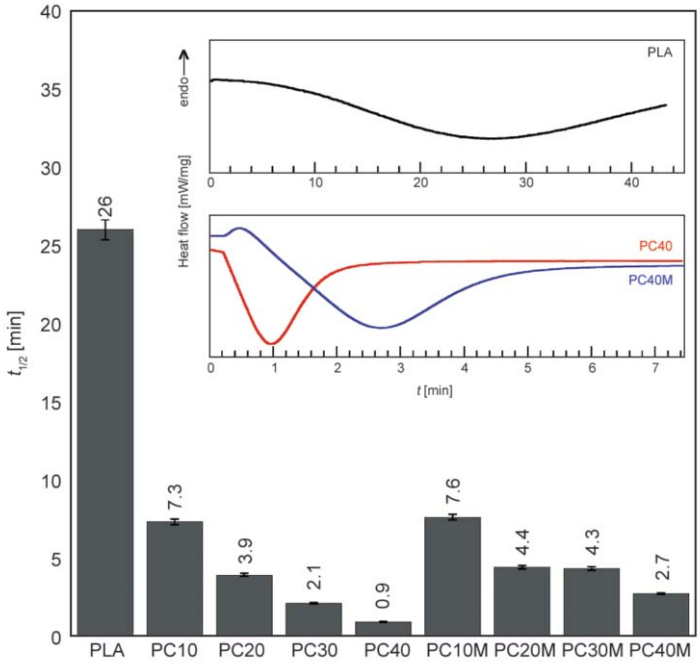

Figure 8. Crystallization half time ($t_{1/2}$) at 100 °C of the PLA and PLA/$CaCO_3$ composites with and without MBS obtained from the isothermal DSC thermogram enclosed with the DSC isothermal curves.

$CaCO_3$ particles [33, 37]. Although the addition of $CaCO_3$ improved the HDT value of PLA, this still limits the use of PLA for high-temperature applications such as microwavable food packaging, automotive interior part or outdoor furniture. For the high heat resistance PLA product manufacturing, longer injection molding cycle time, higher mold temperature or annealing process are recommended for these formulations.

4. Conclusions

In this research, PLA was modified by a toughening agent and a reinforcing filler. Overall, the enhancements of both the toughness and crystallization of PLA with $CaCO_3$ and MBS were successfully observed. The X_c, HDT, tensile strength and impact strength were all increased. Moreover, $t_{1/2}$ significantly reduced from 26 to 0.9 and 2.7 min for PC40 and PC40M respectively. The maximum increment of HDT, by around 8 °C, was found for the PLA with 20 wt% $CaCO_3$. However, this still limits the use of PLA for high-temperature application. For the high heat resistance PLA manufacturing, longer injection molding cycle time, higher mold temperature or annealing process are recommended for these formulations.

Acknowledgements

The authors would like to acknowledge the research grant supported by Srinakharinwirot University (Contract no. 030/2560). Thanks are extended to Mr. Kittisak Phromsuk, Miss Chantaka Nasom, and Mr. Tantai Hongsuwan for their assistance.

References

[1] Petchwattana N., Sanetuntikul J., Narupai B.: Plasticization of biodegradable poly(lactic acid) by different triglyceride molecular sizes: A comparative study with glycerol. Journal of Polymers and the Environment, **26**, 1160–1168 (2018). https://doi.org/10.1007/s10924-017-1012-7

[2] Deng Y., Yu C., Wongwiwattana P., Thomas N-L.: Optimising ductility of poly(lactic acid)/poly(butylene adipate-*co*-terephthalate) blends through *co*-continuous phase morphology. Journal of Polymers and the Environment, **26**, 3802–3816 (2018). https://doi.org/10.1007/s10924-018-1256-x

[3] Petchwattana N., Naknaen P., Narupai B.: A circular economy use of waste wood sawdust for wood plastic composite production: Effect of bio-plasticiser on the toughness. International Journal of Sustainable Engineering, in press (2019). https://doi.org/10.1080/19397038.2019.1688422

[4] Petchwattana N., Naknaen P., Sanetuntikul J., Narupai B.: Crystallisation behaviour and transparency of poly (lactic acid) nucleated with dimethylbenzylidene sorbitol. Plastics, Rubber and Composites, **47**, 147–155 (2018). https://doi.org/10.1080/14658011.2018.1447338

[5] Kasuga T., Maeda H., Kato K., Nogami M., Hata K-I., Ueda M.: Preparation of poly(lactic acid) composites containing calcium carbonate (vaterite). Biomaterials, **24**, 3247–3253 (2003). https://doi.org/10.1016/S0142-9612(03)00190-X

[6] Petchwattana N., Covavisaruch S.: Mechanical and morphological properties of wood plastic biocomposites prepared from toughened poly(lactic acid) and rubber wood sawdust (*Hevea brasiliensis*). Journal of Bionic Engineering, **11**, 630–637 (2014). https://doi.org/10.1016/S1672-6529(14)60074-3

[7] Fonseca C., Ochoa A., Ulloa M. T., Alvarez E., Canales D., Zapata P. A.: Poly(lactic acid)/TiO_2 nanocomposites as alternative biocidal and antifungal materials. Materials Science and Engineering: C, **57**, 314–320 (2015). https://doi.org/10.1016/j.msec.2015.07.069

[8] Dzul-Cervantes M., Herrera-Franco P-J., Tábi T., Valadez-Gonzalez A.: Using factorial design methodology to assess PLA-*g*-Ma and henequen microfibrillated cellulose content on the mechanical properties of poly(lactic acid) composites. International Journal of Polymer Science, **2017**, 4046862/1–4046862/14 (2017). https://doi.org/10.1155/2017/4046862

[9] Zhu J., Xue L., Wei W., Mu C., Jiang M., Zhou Z.: Modification of lignin with silane coupling agent to improve the interface of poly(L-lactic) acid/lignin composites. BioResources, **10**, 4315–4325 (2015). https://doi.org/10.15376/biores.10.3.4315-4325

[10] Petchwattana N., Channuan W., Naknaen P., Narupai B.: 3D printing filaments prepared from modified poly (lactic acid)/teak wood flour composites: An investigation on the particle size effects and silane coupling agent compatibilisation. Journal of Physical Science, **30**, 169–188 (2019). https://doi.org/10.21315/jps2019.30.2.10

[11] Battegazzore D., Frache A., Abt T., Maspoch M. L.: Epoxy coupling agent for PLA and PHB copolymer-based cotton fabric bio-composites. Composites Part B: Engineering, **148**, 188–197 (2018). https://doi.org/10.1016/j.compositesb.2018.04.055

[12] Nagarajan V., Mohanty A-K., Misra M.: Blends of polylactic acid with thermoplastic copolyester elastomer: Effect of functionalized terpolymer type on reactive toughening. Polymer Engineering and Science, **58**, 280–290 (2018). https://doi.org/10.1002/pen.24566

[13] Zhang C., Wang W., Huang Y., Pan Y., Jiang L., Dan Y., Luo Y., Peng Z.: Thermal, mechanical and rheological properties of polylactide toughened by expoxidized natural rubber. Materials and Design, **45**, 198–205 (2013). https://doi.org/10.1016/j.matdes.2012.09.024

[14] Meng B., Deng J., Liu Q., Wu Z., Yang W.: Transparent and ductile poly(lactic acid)/poly(butyl acrylate) (PBA) blends: Structure and properties. European Polymer Journal, **48**, 127–135 (2012). https://doi.org/10.1016/j.eurpolymj.2011.10.009

[15] Petchwattana N., Covavisaruch S., Euapanthasate N.: Utilization of ultrafine acrylate rubber particles as a toughening agent for poly(lactic acid). Materials Science and Engineering: A, **532**, 64–70 (2012). https://doi.org/10.1016/j.msea.2011.10.063

[16] Saeed U., Nawaz M-A., Al-Turaif H-A.: Wood flour reinforced biodegradable PBS/PLA composites. Journal of Composite Materials, **52**, 2641–2650 (2018). https://doi.org/10.1177/0021998317752227

[17] Battegazzore D., Bocchini S., Frache A.: Crystallization kinetics of poly(lactic acid)-talc composites. Express Polymer Letters, **5**, 849–858 (2011). https://doi.org/10.3144/expresspolymlett.2011.84

[18] Yang Y., Zhang L., Xiong Z., Tang Z., Zhang R., Zhu J.: Research progress in the heat resistance, toughening and filling modification of PLA. Science China Chemistry, **59**, 1355–1368 (2016). https://doi.org/10.1007/s11426-016-0222-7

[19] Kim H-S., Park B-H., Choi J-H., Yoon J-S.: Mechanical properties and thermal stability of poly(L-lactide)/calcium carbonate composites. Journal of Applied Polymer Science, **109**, 3087–3092 (2008). https://doi.org/10.1002/app.28229

[20] Nagarajan V., Mohanty A. K., Misra M.: Perspective on polylactic acid (PLA) based sustainable materials for durable applications: Focus on toughness and heat resistance. ACS Sustainable Chemistry and Engineering, **4**, 2899–2916 (2016). https://doi.org/10.1021/acssuschemeng.6b00321

[21] Jiang L., Zhang J., Wolcott M-P.: Comparison of polylactide/nano-sized calcium carbonate and polylactide/montmorillonite composites: Reinforcing effects and toughening mechanisms. Polymer, **48**, 7632–7644 (2007). https://doi.org/10.1016/j.polymer.2007.11.001

[22] Osman M-A., Atallah A., Suter U-W.: Influence of excessive filler coating on the tensile properties of LDPE–calcium carbonate composites. Polymer, **45**, 1177–1183 (2004). https://doi.org/10.1016/j.polymer.2003.12.020

[23] Fuentes C-A., Brughmans G., Tran L. Q. N., Dupont-Gillain C., Verpoest I., van Vuure A-W.: Mechanical behaviour and practical adhesion at a bamboo composite interface: Physical adhesion and mechanical interlocking. Composites Science and Technology, **109**, 40–47 (2015). https://doi.org/10.1016/j.compscitech.2015.01.013

[24] Battegazzore D., Abt T., Maspoch M. L., Frache A.: Multilayer cotton fabric bio-composites based on PLA and PHB copolymer for industrial load carrying applications. Composites Part B: Engineering, **163**, 761–768 (2019). https://doi.org/10.1016/j.compositesb.2019.01.057

[25] Akbari A., Jawaid M., Hassan A., Balakrishnan H.: Epoxidized natural rubber toughened polylactic acid/talc composites: Mechanical, thermal, and morphological properties. Journal of Composite Materials, **48**, 769–781 (2014). https://doi.org/10.1177/0021998313477461

[26] Battegazzore D., Bocchini S., Alongi J., Frache A.: Rice husk as bio-source of silica: Preparation and characterization of PLA–silica bio-composites. RSC Advances, **4**, 54703–54712 (2014). https://doi.org/10.1039/C4RA05991C

[27] Kang K. S., Lee S. I., Lee T. J., Narayan R., Shin B. Y.: Effect of biobased and biodegradable nucleating agent on the isothermal crystallization of poly(lactic acid). Korean Journal of Chemical Engineering, **25**, 599–608 (2008). https://doi.org/10.1007/s11814-008-0101-7

[28] Xu W., He P.: Isothermal crystallization behavior of polyoxymethylene with and without nucleating agents. Journal of Applied Polymer Science, **80**, 304–310 (2001). https://doi.org/10.1002/1097-4628(20010411)80:2<304::AID-APP1100>3.0.CO;2-N

[29] Alata H., Hexig B., Inoue Y.: Effect of poly(vinyl alcohol) fine particles as a novel biodegradable nucleating agent on the crystallization of poly(3-hydroxybutyrate). Journal of Polymer Science Part B: Polymer Physics, **44**, 1813–1820 (2006). https://doi.org/10.1002/polb.20846

[30] Kawamoto N., Sakai A., Horikoshi T., Urushihara T., Tobita E.: Nucleating agent for poly(L-lactic acid) – An optimization of chemical structure of hydrazide compound for advanced nucleation ability. Journal of Applied Polymer Science, **103**, 198–203 (2007). https://doi.org/10.1002/app.25109

[31] Samthong C., Kunanusont N., Deetuam C., Wongkhan T., Supannasud T., Somwangthanaroj A.: Effect of acrylonitrile content of acrylonitrile butadiene rubber on mechanical and thermal properties of dynamically vulcanized poly(lactic acid) blends. Polymer International, **68**, 2004–2016 (2019). https://doi.org/10.1002/pi.5912

[32] Liang J-Z., Zhou L., Tang C-Y., Tsui C-P.: Crystalline properties of poly(L-lactic acid) composites filled with nanometer calcium carbonate. Composites Part B: Engineering, **45**, 1646–1650 (2013). https://doi.org/10.1016/j.compositesb.2012.09.086

[33] Petchwattana N., Covavisaruch S., Petthai S.: Influence of talc particle size and content on crystallization behavior, mechanical properties and morphology of poly (lactic acid). Polymer Bulletin, **71**, 1947–1959 (2014). https://doi.org/10.1007/s00289-014-1165-7

[34] Murariu M., Dubois P.: PLA composites: From production to properties. Advanced Drug Delivery Reviews, **107**, 17–46 (2016). https://doi.org/10.1016/j.addr.2016.04.003

[35] Petchwattana N., Narupai B.: Synergistic effect of talc and titanium dioxide on poly(lactic acid) crystallization: An investigation on the injection molding cycle time reduction. Journal of Polymers and the Environment, **27**, 837–7846 (2019). https://doi.org/10.1007/s10924-019-01396-0

[36] Xia X., Shi X., Liu W., Zhao H., Li H., Zhang Y.: Effect of flax fiber content on polylactic acid (PLA) crystallization in PLA/flax fiber composites. Iranian Polymer Journal, **26**, 693–702 (2017). https://doi.org/10.1007/s13726-017-0554-9

[37] Gao X., Liu R., Jin M., Bu H.: Crystallization and morphology of poly(ethylene-2,6-naphthalene dicarboxylate) in the presence of nucleating agents. Journal of Polymer Science Part B: Polymer Physics, **40**, 2387–2394 (2002). https://doi.org/10.1002/polb.10296